

UNCLASSIFIED

AD NUMBER

AD144762

LIMITATION CHANGES

TO:

Approved for public release; distribution is unlimited. Document partially illegible.

FROM:

Distribution authorized to U.S. Gov't. agencies only; Administrative/Operational Use; SEP 1957. Other requests shall be referred to Office of Naval Research, 875 N. Randolph Street, Arlington, VA 22203-1995. Document partially illegible.

AUTHORITY

ONR ltr, 13 Sep 1977

THIS PAGE IS UNCLASSIFIED

THIS REPORT HAS BEEN DELIMITED
AND CLEARED FOR PUBLIC RELEASE
UNDER DOD DIRECTIVE 5200.20 AND
NO RESTRICTIONS ARE IMPOSED UPON
ITS USE AND DISCLOSURE.

DISTRIBUTION STATEMENT A

APPROVED FOR PUBLIC RELEASE;
DISTRIBUTION UNLIMITED.

**Best
Available
Copy**

UNCLASSIFIED

**A
D 144762**

Armed Services Technical Information Agency

Reproduced by

DOCUMENT SERVICE CENTER

KNOTT BUILDING, DAYTON, 2, OHIO

**FOR
MICRO-CARD
CONTROL ONLY**

1 OF 1

NOTICE: WHEN GOVERNMENT OR OTHER DRAWINGS, SPECIFICATIONS OR OTHER DATA ARE USED FOR ANY PURPOSE OTHER THAN IN CONNECTION WITH A DEFINITELY RELATED GOVERNMENT PROCUREMENT OPERATION, THE U. S. GOVERNMENT THEREBY INCURS NO RESPONSIBILITY, NOR ANY OBLIGATION WHATSOEVER; AND THE FACT THAT THE GOVERNMENT MAY HAVE FORMULATED, FURNISHED, OR IN ANY WAY SUPPLIED THE SAID DRAWINGS, SPECIFICATIONS, OR OTHER DATA IS NOT TO BE REGARDED BY IMPLICATION OR OTHERWISE AS IN ANY MANNER LICENSING THE HOLDER OR ANY OTHER PERSON OR CORPORATION, OR CONVEYING ANY RIGHTS OR PERMISSION TO MANUFACTURE, USE OR SELL ANY PATENTED INVENTION THAT MAY IN ANY WAY BE RELATED THERETO.

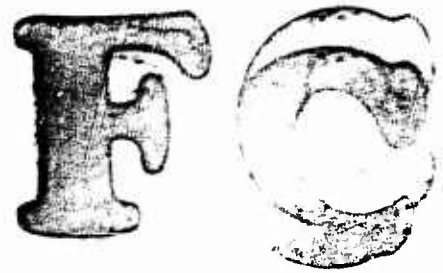
UNCLASSIFIED

AD W0144762
ASIA RE COPY

OFFICE OF NAVAL RESEARCH

Contract Nonr-562(10)

NR-064-406



Technical Report No. 28

**STRAIN-HARDENING AND STRAIN-RATE EFFECTS
IN THE IMPACT LOADING OF CANTILEVER BEAMS**

by

G. R. Cowper and P. S. Symonds

DIVISION OF APPLIED MATHEMATICS

BROWN UNIVERSITY

PROVIDENCE, R. I.

September 1957

C11-28

Reproduction in whole or in part is permitted for any purpose
of the United States Government.

STRAIN-HARDENING AND STRAIN-RATE EFFECTS
IN THE
IMPACT LOADING OF CANTILEVER BEAMS¹

by

G. R. Cowper² and F. C. Symonds³

Abstract. The problem of impact loading of a cantilever beam which exhibits either strain-hardening or strain-rate sensitivity is considered. On the basis of an assumption concerning the mode of deformation of the beam, the motion of the beam is analysed. The influence of strain-hardening and strain-rate sensitivity on the permanent deformation is calculated. In addition, numerical results are presented for the predicted plastic strains and strain-rates within the beam. Finally, directions in which an extension of the analysis is desirable, are indicated.

-
1. The results presented in this paper were obtained in the course of research sponsored by the Office of Naval Research under Contract Nonr-562(10) with Brown Univ.
 2. Research Assistant, Division of Applied Mathematics, Brown University, Providence 12, Rhode Island.
 3. Professor of Engineering, Brown University.

List of Symbols

A, dA	area and element of area of cross-section of beam
c	distance from neutral axis to extreme fibre of beam
D	coefficient in $\sigma - \dot{\epsilon}$ relation
D'	coefficient in moment-curvature relation
E	Young's modulus
$F(\eta)$	$\equiv 2\eta + \eta^2 + (1 + \eta)\sqrt{(1 + \eta)^2 - 1} - \ln(1 + \eta - \sqrt{(1 + \eta)^2 - 1})$
G	mass at tip of beam
$H(\rho)$	$\equiv \frac{1}{\rho^2} + \ln \rho^2 - 1$
I	moment of inertia of cross-section of beam
K	$= \frac{G}{m\ell} = \text{ratio } \frac{\text{tip mass}}{\text{beam mass}}$
ℓ	length of beam
m	<div style="display: flex; align-items: center;"> <div style="font-size: 3em; margin-right: 10px;">{</div> <div> <p>(1) mass per unit length of beam</p> <p>(2) as subscript, denotes quantities pertaining to the root of the beam</p> </div> </div>
M	bending moment
M_0	static limit moment of beam
n	ratio $\frac{E}{(d\sigma/d\epsilon)_{pl}}$ of slopes of elastic and plastic parts of σ - ϵ curve
p	exponent in stress-strain-rate relation
Q	shearing force in beam
R	ratio $\frac{\text{initial kinetic energy}}{\text{maximum elastic strain energy}}$
S	ratio M_m/M_0
S_0	initial value of S

- t time, measured from instant of impact
- u dummy variable of integration
- v impact velocity of beam
- x distance along beam, measured from root
- x_p distance from root of beam to end of plastic region
- x_0 maximum value of x_p
- y deflection of beam
- z distance from neutral axis to a generic point of the beam
- Z_0 plastic section modulus of beam
- α abbreviation for $\frac{1}{2} \left(\frac{1-6K}{2-6K} \right) = \frac{EI}{nW_0 J} \left(\frac{1-6K}{2-6K} \right)$
- β coefficient in moment-curvature relation
- $\Gamma(\cdot)$ gamma function
- ϵ strain
- ξ dummy variable of integration
- η abbreviation for $\alpha \theta_p = \frac{EI}{nW_0 J} \left(\frac{1-6K}{2-6K} \right) \theta_p$
- θ angle of deflection of straight part of beam
- θ_p damage angle = maximum value of θ
- θ_0 damage angle for beam of ideally plastic material
- κ curvature of beam = $\frac{\partial^2 y}{\partial x^2}$
- λ strain-hardening coefficient in moment-curvature relation
- ζ dummy variable of integration
- ρ parameter defined by $\rho = 1 + \alpha - \sqrt{(1 + \alpha)^2 - 1}$
- σ stress, in particular longitudinal bending stress in beam

- σ_0 static yield stress
 φ slope of beam = $\frac{\partial y}{\partial x}$
• dot denotes differentiation with respect to time

1. Introduction. We consider a uniform cantilever beam with attached tip mass moving initially with velocity V normal to its length. At time $t=0$ the root of the beam is instantaneously brought to rest by contact with a rigid stop. (See Fig. 1). The problem is to determine the subsequent motion of the beam and, particularly, its permanent plastic deformation. Interest in this problem stems from the fact that it represents a case in which the plastic deformation of beams under impact loading can be conveniently investigated experimentally.

Lee and Symonds [1] showed that a comparatively simple theoretical analysis of problems of dynamic loading of beams is possible if it is assumed that the beam is made of a rigid-ideally-plastic material. This rigid-ideally-plastic analysis was further developed by Symonds and Leth [2] and by Mentel [3]. In addition, experimental investigations of the problem have been carried out at Brown University, and the results have been reported by Symonds, Green and Mentel [4], and by Mentel [3]. Large quantitative discrepancies were found between theory and experiment. Mentel [3] attributed the discrepancy to strain-hardening and strain-rate effects which are neglected in the rigid-ideally plastic analysis.

Impact tests made by Parkes [5] showed similar discrepancies with the elementary rigid-ideally plastic analysis. Parkes showed that a simple correction made for a strain rate effect alone led to good agreement. Both Mentel and Parkes used a value of limit moment which was constant in any one case, but multiplied by a factor to take account of rate of strain. While their method of correction gives the right magnitudes of corrections needed in the cases studied its general validity seems highly uncertain.

It therefore seems desirable to extend the theoretical treatment of the problem to include strain-hardening and strain-rate effects. The present report is an attempt to make this extension. Theoretical analyses are presented for beams which exhibit either strain-hardening, or strain-rate sensitivity, separately. The influence of these effects on the permanent plastic deformation is studied. In addition, expressions are derived for the magnitudes of the plastic strains and strain-rates which occur in the beam, and numerical results are presented which apply to the beams used in the experiments [3, 4].

2. General Analysis.

2.1 Stress-Strain Relations. Two stress-strain relations for the plastic range are considered:

$$\sigma = \sigma_0 + \frac{E}{n} \epsilon, \quad \sigma > \sigma_0 \quad (1)$$

$$\dot{\epsilon} = D (\sigma - \sigma_0)^P, \quad \sigma > \sigma_0 \quad (2)$$

Relation (1) introduces linear strain-hardening as illustrated in Fig. 2. Note that the constant n can be interpreted as the ratio of the slopes of the elastic and plastic portions of the stress-strain curve. Relation (2) introduces a strain-rate effect but no strain hardening. This particular form of the stress-strain relation is suggested by the experimental data of Nadai and Manjoine on the dependence of the yield stress on the rate of straining [5, 6]. By suitable choice of D and p , relation (2) can be made to agree closely with experimental σ - $\dot{\epsilon}$ curves. This is shown in Fig. 5, which compares the experimental σ - $\dot{\epsilon}$ curve for mild steel with relation (2).

In this analysis elastic strains are neglected; the material is assumed rigid when the stress is less than the static yield stress σ_0 . According to references [1] and [2] the criterion for the validity of this assumption is that the beam's initial kinetic energy should greatly exceed the maximum elastic strain energy which can be stored in the beam. The criterion is satisfied for all applications which we make of the present theory.

In order to develop moment-curvature relations from the stress-strain relations, the usual assumptions of beam theory are made. Thus we assume that plane cross-sections normal to the centre-line remain plane and normal to the centre-line during bending; that the cross-section has two

perpendicular axes of symmetry and bending takes place about one of them; that the material has the same properties in tension and compression, etc. Then the strain and strain rate at any point of a cross-section are

$$\varepsilon = \kappa z \quad \dot{\varepsilon} = \dot{\kappa} z$$

where z is the distance from the neutral axis. With this result, and the stress-strain relations, the bending moment

$$M = \int_{-c}^c z \sigma(z) dA$$

at any section can be calculated and hence the moment-curvature relations are obtained. For the stress-strain relations (1) and (2) the corresponding moment-curvature relations are, respectively

$$M = M_0 (1 - \lambda \kappa), \quad M > M_0 \quad (3)$$

$$\dot{\kappa} = D' (M - M_0)^p, \quad M > M_0 \quad (4)$$

where

$$M_0 = \sigma_0 Z_0 \quad \lambda = \frac{EI}{nM_0}$$

and

$$D' = \frac{D}{\left(\int_{-c}^c z^{1+\frac{1}{p}} dA \right)^p}$$

For a rectangular section,

$$D' = \frac{D}{Z_0^p} \frac{(2p+1)^p}{2p}$$

The stress-strain relations (1) and (2) can be regarded as special cases of a more general relation. Malvern [7] has suggested the form for the σ - ϵ - $\dot{\epsilon}$ relation

$$\dot{\epsilon} - \frac{\dot{\sigma}}{E} = g(\sigma - f(\epsilon)) \quad (5)$$

where $\sigma = f(\epsilon)$ is the static stress-strain relation. Thus, the plastic strain rate is a function of the "excess stress" $\sigma - f(\epsilon)$. If elastic strains are neglected the term $\dot{\sigma}/E$ can be deleted. The relation

$$\dot{\epsilon} = D(\sigma - \sigma_0 - \frac{E}{n} \epsilon)^p$$

is a special form of (5), and includes the relations (1) and (2) as special cases. The corresponding moment-curvature relation is

$$\dot{\kappa} = D'(M - M_0(1 + \lambda\kappa))^p$$

2.2 Equations of Motion. While plastic deformation of an ideally-plastic beam is concentrated at certain points (plastic hinges), the regions of plastic flow in a strain-hardening or rate-sensitive material can be expected to be of finite length. This, plus the fact that the position and extent of the plastic regions are not a priori known, would greatly complicate the analysis, were it not for experimental evidence which suggests that some simplifying approximations are permissible. From the tests carried out by Mentel, Green, and Symonds [4], it appears that:

- (1) plastic flow occurs only in a region adjacent to the root of the beam,
- (2) the length of the plastic region is short compared with the length of the beam,
- (3) bending takes place in one sense only; that is, the bending moment in the plastic region always has the same sign.

Thus, with the 5 inch long beam specimens tested by Mentel, Green, and Symonds, only that part of the beam within about $3/4$ inch of the root was permanently bent after impact. Outside this region the beam specimens appeared to remain straight and unbent.

The above experimental evidence may not, at first sight, seem to be in harmony with the analyses of Lee and Symonds [1], or Symonds and Leth [2], who show that two plastic hinges, one at the root and one in the interior, are to be expected, and that the senses of rotation at each hinge are opposite to each other. However, Mentel [3] has shown that the effect of the interior hinge is often negligibly small, especially if K is large. Thus the rigid-ideally-plastic theory also indicates that plastic flow is essentially confined to the root of the beam.

In view of this evidence we assume that the motion of the beam after impact is approximately a rigid-body rotation about the root, and we assume that, for the purpose of deriving the equations of motion, the region of plastic flow can

be adequately represented by a point hinge. Then, treating the entire beam as a rigid body, and referring to Fig. 3, we find that the equations of linear and angular momentum are

$$Q_m = - \left(\frac{1}{2} m l^2 + G \right) \ddot{\theta} = - \frac{m l^2}{2} (1 + 2K) \ddot{\theta} \quad (6)$$

$$M_m = - \left(\frac{1}{3} m l^3 + G l \right) \ddot{\theta} = - \frac{m l^3}{3} (1 + 3K) \ddot{\theta} \quad (7)$$

2.3 Initial Conditions. It will be necessary to know initial values of θ and $\dot{\theta}$.

Clearly, the value of θ at the instant of impact is $\theta(0) = 0$. To find the initial value of $\dot{\theta}$ we use the fact that the angular momentum about the root suffers no impulsive change at the instant of impact. This is so because the bending moment M_m is limited to finite values, while the impulsive shear force Q_m , although possibly infinite at the instant of contact, produces no torque about the root of the beam. Hence no impulsive torque acts at the instant of impact. Equating angular momenta of the beam about its root before and after impact gives

$$\frac{m l^2 v}{2} + G l v = \frac{m l^3 \dot{\theta}(0)}{3} + G l \dot{\theta}(0)$$

whence

$$\dot{\theta}(0) = \frac{v}{l} \left(\frac{3+6K}{2+6K} \right) \quad (8)$$

2.4 Moment-Angle Relation across Plastic Region. At a particular instant, let plastic flow be confined to the region $0 \leq x \leq x_n$, as shown in Fig. 4. x_n is, of course a function of time. For $x > x_n$, the beam is rigid. If x_0 is the largest value of x_n , then for $x > x_0$ the beam remains straight. The slope at any point of the beam is given by

$$\begin{aligned}\varphi &= \int_0^x d\varphi = \int_0^x \frac{\partial \varphi}{\partial x} dx \\ &= \int_0^x \kappa dx\end{aligned}$$

In particular,

$$\varphi = \int_0^{x_0} \kappa dx = \int_0^{x_n} \kappa dx + \int_{x_n}^{x_0} \kappa dx \quad (9)$$

Differentiation of (9) gives the angular velocity of the straight part of the beam,

$$\dot{\varphi} = \int_0^{x_0} \dot{\kappa} dx = \int_0^{x_n} \dot{\kappa} dx \quad (10)$$

since $\dot{\kappa} = 0$ for $x > x_n$.

If rotatory inertia is neglected, the shear force and bending moment satisfy the equations of motion

$$\frac{\partial Q}{\partial x} = m\ddot{y} \quad \frac{\partial M}{\partial x} = -Q \quad (11)$$

Now deflections near the root are small, and it is reasonable to suppose that accelerations near the root are small

also. Thus, we assume that \ddot{y} is so small within the plastic region that the term $m\ddot{y}$ may be neglected in comparison with $\frac{\partial Q}{\partial x}$. Then

$$\frac{\partial Q}{\partial x} = 0$$

whence

$$Q = Q_m$$

for $0 \leq x \leq x_n$. Further,

$$\frac{\partial M}{\partial x} = Q_m$$

$$M = -Q_m x + C(t)$$

for $0 \leq x \leq x_n$. At the boundary of the plastic region $M=M_0$; that is $M=M_0$ when $x=x_n$. Hence

$$M = M_0 + (x_n - x) Q_m \quad (12)$$

Putting $x=0$, we find

$$M_m = M_0 + x_n Q_m$$

or

$$x_n = \frac{M_m - M_0}{Q_m} \quad (13)$$

From (12) we note that, within the plastic region,

$$dx = -\frac{dM}{Q_m} \quad (14)$$

Substitution of this result into (10) leads to

$$\dot{\theta} = \frac{-1}{Q_m} \int_{x=0}^{x=x_n} \dot{x} dM = \frac{-1}{Q_m} \int_{M=M_m}^{M=M_0} \dot{x} dM \quad (15)$$

If \dot{x} is a function of M only, then (15) can be evaluated to give a relation between $\dot{\theta}$, M_m , and Q_m . This relation, together with the two equations of motion, (6) and (7), is sufficient for an analysis of the motion of the beam.

From (9) and (14),

$$\theta = \frac{-1}{Q_m} \left\{ \int_{x=0}^{x=x_n} x dM + \int_{x=x_n'}^{x=x_0} x dM \right\}.$$

If x_n is an increasing function of time, then $x=0$ for $x > x_n$ and hence

$$\theta = \frac{-1}{Q_m} \int_{M=M_m}^{M=M_0} x dM \quad (16)$$

This integral can be evaluated if x is a function of M only. Again, this relation, plus the two equations of motion, (6) and (7), are sufficient for an analysis of the motion of the beam.

To investigate whether x_n is an increasing or decreasing function of time, consider

$$\begin{aligned} x_n &= \frac{M_m - M_0}{Q_m} \\ &= \frac{2}{3+6K} + \frac{2M_0}{m\ell^2(1+2K)\ddot{\theta}} \end{aligned} \quad (17)$$

which is obtained by substituting for M_m and Q_m from (6) and (7) into (13). Note that $\ddot{\theta}$ is a negative quantity.

For a strain hardening beam, M_m will increase with θ and with time, and hence the deceleration $\ddot{\theta}$ will also increase

in absolute value with time. Then it follows from (17) that x_n is an increasing function of time.

For a rate-sensitive beam, velocities and strain-rates can be expected to decrease with time, and hence so will M_m . Therefore the deceleration $\ddot{\theta}$ will decrease in absolute value with time. Hence, from (17) x_n is a decreasing function of time in this case.

It follows that formula (16) may be used for a strain-hardening beam. For a beam which exhibits both strain-hardening and strain rate effects, however, it is not clear how x_n changes with time, and hence it is uncertain whether formula (16) applies.

3. Analysis for Strain-Hardening Beam.

3.1 Calculation of Damage Angle θ_f . Here the moment-curvature relation is (3), namely

$$M = M_0(1 + \lambda \kappa), \quad M > M_0$$

or

$$\kappa = \frac{M - M_0}{\lambda M_0}$$

Substituting this into (16) and integrating, we obtain the relation

$$\theta = \frac{(M_m - M_0)^2}{2\lambda Q_m M_0} \quad (18)$$

Elimination of Q_m between (18) and the equation of motion (6) and (7) leads to the equations

$$\left. \begin{aligned} \theta &= \left(\frac{2+6K}{3+6K} \right) \frac{l}{2\lambda} \frac{(S-1)^2}{S} \\ \ddot{\theta} &= - \frac{6M_0}{m l^3 (2+6K)} S \end{aligned} \right\} \quad (19)$$

where $S \equiv M_m/M_c$. Solving the first of equations (19) for S we obtain

$$S = (1 + \alpha\theta) \pm \sqrt{(1 + \alpha\theta)^2 - 1} \quad (20)$$

where

$$\alpha = \frac{\lambda}{l} \left(\frac{3+6K}{2+6K} \right) = \frac{EI}{nM_0 l} \left(\frac{3+6K}{2+6K} \right)$$

Substitution of (20) into the second of equations (19) gives

$$\ddot{\theta} = - \frac{6M_0}{m l^3 (2+6K)} \left\{ (1 + \alpha\theta) \pm \sqrt{(1 + \alpha\theta)^2 - 1} \right\} \quad (21)$$

As θ increases so does M_m , because of the strain hardening and consequently the angular deceleration of the beam increases also. This shows that the positive sign must be chosen in (21).

Now

$$2\ddot{\theta} = 2 \frac{d\dot{\theta}}{dt} = 2\dot{\theta} \frac{d\dot{\theta}}{d\theta} = \frac{d}{d\theta} (\dot{\theta}^2) \quad (22)$$

and hence, from (21) and (22),

$$\frac{d(\dot{\theta}^2)}{d\theta} = - \frac{12M_0}{m l^3 (2+6K)} \left\{ 1 + \alpha\theta + \sqrt{(1 + \alpha\theta)^2 - 1} \right\} d\theta \quad (23)$$

The damage angle θ_f is found by integrating (23). The limits of integration are: at the beginning of motion $\theta = 0$ and $\dot{\theta} = \frac{V}{l} \left(\frac{3+6K}{2+6K} \right)$; the motion ceases when $\dot{\theta} = 0$, at which time $\theta = \theta_f$. Hence

$$\int_{\dot{\theta} = \frac{V}{l} \left(\frac{3+6K}{2+6K} \right)}^{\dot{\theta}=0} d(\dot{\theta}^2) = \frac{-12M_0}{m l^3 (2+6K)} \int_0^{\theta_f} \left\{ 1 + \alpha \dot{\theta} + \sqrt{(1 + \alpha \theta)^2 - 1} \right\} d\theta$$

or

$$\frac{m E I V^2}{12 n M_0^2} \frac{(3 + 6K)^3}{(2 + 6K)^2} = \int_0^{\alpha \theta_f} \left\{ 1 + \xi + \sqrt{(1 + \xi)^2 - 1} \right\} d\xi$$

$$= \int_0^{\eta} \left\{ 1 + \xi + \sqrt{(1 + \xi)^2 - 1} \right\} d\xi \quad (24)$$

where

$$\xi = \alpha \theta$$

$$\eta = \alpha \theta_f = \frac{E I}{n M_0 l} \left(\frac{3 + 6K}{2 + 6K} \right) \theta_f \quad (25)$$

Now

$$\int_0^{\eta} \left\{ 1 + \xi + \sqrt{(1 + \xi)^2 - 1} \right\} d\xi$$

$$= \frac{1}{2} \left\{ 2\eta + \eta^2 + (1+\eta) \sqrt{(1+\eta)^2 - 1} - \ln(1+\eta + \sqrt{(1+\eta)^2 - 1}) \right\}$$

$$= \frac{1}{2} F(\eta) \quad (26)$$

Then (24) becomes

$$\begin{aligned}
 F(\eta) &= \frac{mEI V^2}{6nM_0^2} \frac{(3 + 6K)^3}{(2 + 6K)^2} \\
 &= \frac{9}{8} \frac{mEI V^2}{nM_0^2} \frac{(1 + 2K)^3}{(1 + 3K)^2}
 \end{aligned} \tag{27}$$

and (25) may be written, using (27)

$$\frac{\theta_f}{\theta_0} = \frac{2\eta}{F(\eta)} \tag{28}$$

where

$$\theta_0 = \frac{3}{8} \frac{mEI V^2}{M_0} \frac{(1 + 2K)^2}{(1 + 3K)} \tag{29}$$

is the damage angle which would be obtained if the beam were ideally plastic. Relation (29) is derived in reference [4].

Equations (27) and (28) give the relation between

θ_f/θ_0 and the non-dimensional velocity $\frac{mEI V^2}{nM_0^2} \frac{(1 + 2K)^3}{(1 + 3K)^2}$. This

relation is plotted in figure 6, together with experimentally determined points taken from the data of reference [3].

In order to plot the experimental points an estimate of the value of n is needed, which is obtained as follows. We take the slope of the post-yield portion of the stress-strain curve to be approximately

$$\frac{\sigma_{ULT} - \sigma_0}{\epsilon_{ULT}}$$

where σ_{ULT} is the ultimate stress of the metal and ϵ_{ULT} the corresponding fractional elongation. Then

$$n = \frac{E \epsilon_{ULT}}{\sigma_{ULT} - \sigma_0}$$

For the mild steel beams used in the experiments, $\sigma_{ULT} \approx 56,000$ psi., $\sigma_0 \approx 33,000$ psi., $\epsilon_{ULT} \approx 0.1$, whence $n \approx 130$. This value was used in plotting the experimental points of figure 6.

The non-dimensional velocity $\frac{mEIv^2}{nM_0^2} \frac{(1+2K)^3}{(1+3K)^2}$ can be

interpreted in terms of the ratio R of the beams initial kinetic energy to the maximum elastic strain energy which can be stored within the beam. (Recall that it is this ratio which determines whether elastic strains may be neglected.) The expression

for R is

$$R = \frac{\frac{1}{2} mlv^2 + \frac{1}{2} GV^2}{\frac{1}{2} \frac{M_0^2 l}{EI}}$$

$$= \frac{mEIv^2}{M_0^2} (1 + K)$$

and hence

$$\frac{mEIv^2}{nM_0^2} \frac{(1+2K)^3}{(1+3K)^2} = \frac{R}{n} \cdot \left[\frac{(1+2K)^3}{(1+K)(1+3K)^2} \right]$$

The quantity $\left[\frac{(1+2K)^3}{(1+K)(1+3K)^2} \right]$ is plotted in figure 7, and it

can be seen that this quantity is almost constant over most of the practical range of K . Thus the reduction in damage angle due to strain-hardening is chiefly a function of R/n , the parameter K having only a small influence.

3.2. Calculation of Maximum Plastic Strain

The maximum strain occurs at the root of the beam, where the bending moment is greatest.

From (3)

$$\kappa = \frac{1}{\lambda} \left(\frac{M}{M_0} - 1 \right)$$

and hence the curvature at the root of the beam is

$$\begin{aligned} \kappa_m &= \frac{1}{\lambda} \left(\frac{M_m}{M_0} - 1 \right) = \frac{S - 1}{\lambda} \\ &= \frac{\alpha\theta + \sqrt{(1 + \alpha\theta)^2 - 1}}{\lambda} \end{aligned}$$

using (20). The strain at the extreme fibre, at the root, is then

$$\kappa_m c = \frac{c}{\lambda} \left\{ \alpha\theta + \sqrt{(1 + \alpha\theta)^2 - 1} \right\} \quad (29)$$

and the final strain at the end of the deformation is

$$\begin{aligned} \epsilon_m &= \frac{c}{\lambda} \left\{ \alpha\theta_f + \sqrt{(1 + \alpha\theta_f)^2 - 1} \right\} \\ &= \frac{n}{E} \frac{M_0 c}{I} \left\{ \eta + \sqrt{(1 + \eta)^2 - 1} \right\} \quad (31) \end{aligned}$$

Equations (27) and (31) give the relation between the maximum strain and the non-dimensional impact velocity. This relation is plotted in figure 8 using values of the parameters appropriate to the mild-steel beams which were used in the experiments reported in reference [3].

3.3. Calculation of Strain-Rates:

From (30) and (31),

$$\epsilon_m = \frac{nM_o c}{EI} [\alpha\theta + \sqrt{(1 + \alpha\theta)^2 - 1}]$$

and differentiation of this result with respect to time gives

$$\dot{\epsilon}_m = \frac{nM_o c}{EI} \left[1 + \frac{1}{\sqrt{(1 + \alpha\theta)^2 - 1}} \right] \alpha \dot{\theta} \quad (32)$$

Note that as θ tends to zero and $\dot{\theta}$ tends to the initial (finite) angular velocity, then, according to (32), $\dot{\epsilon}_m$ tends to infinity. Thus the present theory predicts that the initial strain-rate is infinite.

The mean strain-rate, i.e. the time average strain-rate at the root of the beam is

$$\dot{\epsilon}_{MEAN} = \frac{\int \dot{\epsilon} dt}{\int dt} = \frac{\epsilon_m}{\int dt} \quad (33)$$

where the integration extends over the time during which plastic flow occurs. To find $\int dt$, return to equation (23) and integrate it between the limits $\ddot{\theta} = \ddot{\theta}$, $\theta = \theta$, and the final values $\ddot{\theta} = 0$, $\theta = \theta_f$. Thus

$$\int_{\ddot{\theta}=\ddot{\theta}}^{\ddot{\theta}=0} d(\dot{\theta}^2) = \frac{-12M_o}{m\ell^3(2 + 6K)} \int_{\theta=\theta}^{\theta=\theta_f} \left\{ 1 + \alpha\theta + \sqrt{(1 + \alpha\theta)^2 - 1} \right\} d\theta$$

whence

$$\dot{\theta}^2 = \frac{6nM_o^2}{mEI\ell^2(3 + 6K)} [F(\eta) - F(\alpha\theta)]$$

using (26) and (25). After solving for $\dot{\theta} = d\theta/dt$, we can obtain

$$dt = \left(\frac{mEI\ell^2(3+6K)}{6nM_0^2} \right)^{\frac{1}{2}} \frac{d\theta}{[F(\eta) - F(\alpha\theta)]^{\frac{1}{2}}}$$

The length of time during which plastic flow occurs then is

$$\begin{aligned} \int dt &= \left(\frac{mEI\ell^2(3+6K)}{6nM_0^2} \right)^{\frac{1}{2}} \int_{\theta=0}^{\theta=\theta_r} [F(\eta) - F(\alpha\theta)]^{-\frac{1}{2}} d\theta \\ &= \left(\frac{m\ell^4}{6EI} \frac{(2+6K)^2}{(3+6K)} \right)^{\frac{1}{2}} \int_{\xi=0}^{\xi=\eta} [F(\eta) - F(\xi)]^{-\frac{1}{2}} d\xi \end{aligned} \quad (34)$$

on substituting $\xi = \alpha\theta$ from (25).

The integral in (34) has to be evaluated numerically. In the above form, however, the integral is not suitable for numerical treatment because of the singularity at the upper limit. This singularity can be removed by integrating once by parts and then making the substitutions

$$\left. \begin{aligned} \zeta &= 1 + \xi - \sqrt{(1 + \xi)^2 - 1} \\ \rho &= 1 + \eta - \sqrt{(1 + \eta)^2 - 1} \end{aligned} \right\} \quad (35)$$

This maneuver reduces (34) to

$$\frac{6M_0}{m\ell^2V(3+6K)} \int dt = 1 - \int_{\rho}^1 \left[1 - \frac{H(\zeta)}{H(\rho)} \right]^{\frac{1}{2}} d\zeta \quad (36)$$

while the substitutions (35) change (26) and (27) to

$$H(\rho) = \frac{9}{4} \frac{mEIV^2}{nM_0^2} \frac{(1+2K)^3}{(1+3K)^2} \quad (37)$$

where

$$H(\rho) \equiv \frac{1}{\rho^2} + \ln \rho^2 - 1 \quad (38)$$

Finally the time-average strain-rate is found using (31), (33), (36), (37), and (38), as

$$\dot{\epsilon}_{\text{MEAN}} = \frac{3c}{l^2} \left[\frac{nM_0^2}{mEI} \frac{(1+2K)}{(1+3K)^2} \right]^{\frac{1}{2}} \frac{(1-\rho)}{\left\{ 1 + \rho^2 \ln \rho^2 - \rho^2 \right\}^{\frac{1}{2}} \left\{ 1 - \int_{\rho}^1 \left[1 - \frac{H(\zeta)}{H(\rho)} \right]^{\frac{1}{2}} d\zeta \right\}} \quad (39)$$

Equations (37) and (39) give the relation between non-dimensional impact velocity and mean strain-rate. This is plotted in figure 9, again using values of the parameters appropriate to the mild-steel beams which were used in the experiments reported in reference [3]. We note that the mean strain-rate depends significantly on K.

3.4. Length of Plastic Region

From the equations of motion (6) and (7) we obtain

$$Q_m = \frac{M_m}{l} \left(\frac{2}{3} + \frac{6K}{6K} \right)$$

and substitution of this result into (13) leads to

$$\frac{x_n}{l} = \left(\frac{2}{3} + \frac{6K}{6K} \right) \frac{S-1}{S} \quad (40)$$

where $S \equiv M_m/M_0$. Substitution for S from (20) gives

$$\frac{x_n}{l} = \left(\frac{2}{3} + \frac{6K}{6K} \right) (-\alpha\theta + \sqrt{(1 + \alpha\theta)^2 - 1})$$

The maximum value of x_n is given by

$$\begin{aligned}
 \max\left(\frac{x_n}{l}\right) &= \left(\frac{2+6K}{3+6K}\right)(-\alpha\theta_f + \sqrt{(1+\alpha\theta_f)^2 - 1}) \\
 &= \left(\frac{2+6K}{3+6K}\right)(-\eta + \sqrt{(1+\eta)^2 - 1}) \quad (41)
 \end{aligned}$$

The value of $\max(\frac{x_n}{l})$ is plotted against the non-dimensional impact velocity in figure 10.

Since it is a basic assumption of the present analysis that x_n/l is small, figure 10 shows that there is an upper limit on the impact velocities for which the present theory is valid. The requirement $x_n/l \ll 1$ will be satisfied provided, say,

$$\frac{mEIV^2}{nM_0^2} \frac{(1+2K)^3}{(1+3K)^2} < .05$$

Recalling from the discussion of section 3.1 that

$$\frac{mEIV^2}{nM_0^2} \frac{(1+2K)^3}{(1+3K)^2} \approx .85 \frac{R}{n}$$

then the requirement can be stated

$$R < .06n$$

For $n = 130$, this becomes $R < 8$, roughly. On the other hand, there is the conflicting requirement $R \gg 1$ which must be satisfied in order that elastic strains may legitimately be neglected. Therefore it appears that the present analysis is valid only for a limited range of R , in the neighborhood of $R = 8$.

4. Analysis for Rate-Sensitive Beam

4.1. Calculation of Damage Angle Θ

Here we use the moment-curvature relation (4), which introduces a strain-rate effect,

$$\begin{aligned}\dot{\kappa} &= D'(M - M_0)^p \\ &= \frac{\beta}{c} \left(\frac{M}{M_0} - 1 \right)^p\end{aligned}\quad (42)$$

where, for a beam of rectangular section,

$$\beta \equiv cD'M_0^p = D\sigma_0^p \left(\frac{2p+1}{2p} \right)^p$$

We note that, in terms of β , the stress-strain relation (2) can be written

$$\dot{\epsilon} = \beta \left(\frac{2p}{2p+1} \right)^p \left(\frac{\sigma}{\sigma_0} - 1 \right)^p$$

From (42) and (15) we find that the moment-angle relation across the plastic zone is

$$\begin{aligned}\dot{\Theta} &= \frac{1}{Q_m} \int_{M_0}^{M_m} \dot{\kappa}(M) dM \\ &= \frac{\beta M_0}{Q_m(p+1)c} \left(\frac{M_m}{M_0} - 1 \right)^p\end{aligned}\quad (43)$$

Elimination of Q_m between the equations of motion (6), (7) and (43) leads to

$$\dot{\Theta} = \frac{\beta \ell}{(p+1)c} \left(\frac{2+6K}{3+6K} \right) \frac{(S-1)^{p+1}}{S} \quad (44)$$

$$\ddot{\Theta} = \frac{-6M_0}{m\ell^3(2+6K)} S \quad (45)$$

where $S \equiv M_m/M_0$. From (44),

$$d\dot{\theta} = \frac{3\ell}{c} \left(\frac{2+6K}{3+6K} \right) \left\{ \frac{(S-1)^p}{S} - \frac{1}{(p+1)} \frac{(S-1)^{p+1}}{S^2} \right\} dS \quad (46)$$

Now

$$\ddot{\theta} = \frac{d\dot{\theta}}{dt} = \frac{d\dot{\theta}}{d\theta} \frac{d\theta}{dt} = \dot{\theta} \frac{d\dot{\theta}}{d\theta}$$

whence

$$d\theta = \frac{\dot{\theta} d\dot{\theta}}{\ddot{\theta}} \quad (47)$$

Substitution from (44), (45), and (46) into (47) yields

$$d\theta = \frac{-m\beta^2 \ell^5}{6(p+1)c^2 M_0} \frac{(2+6K)^3}{(3+6K)^2} \left\{ \frac{(S-1)^{2p+1}}{S^3} - \frac{1}{(p+1)} \frac{(S-1)^{2p+2}}{S^4} \right\} dS \quad (48)$$

The damage angle θ_f is obtained by integrating (48). The limits of integration are obtained from (44). At the beginning of the motion $\theta = 0$ and $\dot{\theta} = \frac{V}{\ell} \left(\frac{3+6K}{2+6K} \right)$. Then, using (44) we find that S_0 , the initial value of S , is given by

$$\frac{(S_0 - 1)^{p+1}}{(p+1)S_0} = \frac{Vc}{\beta \ell^2} \left(\frac{3+6K}{2+6K} \right)^2 \quad (49)$$

The motion ceases when $\dot{\theta} = 0$. When $\dot{\theta} = 0$, then $S = 1$, from (44). Integration of (48) between the limits $\theta = 0$, $S = S_0$ and $\theta = \theta_f$, $S = 1$ gives

$$\begin{aligned} \theta_f &= \frac{-m\beta^2 \ell^5}{6(p+1)c^2 M_0} \frac{(2+6K)^3}{(3+6K)^2} \int_{S_0}^1 \left\{ \frac{(S-1)^{2p+1}}{S^3} - \frac{1}{(p+1)} \frac{(S-1)^{2p+2}}{S^4} \right\} dS \\ &= \theta_0 \frac{2}{(p+1)} \frac{\beta^2 \ell^4}{V^2 c^2} \left(\frac{2+6K}{3+6K} \right)^4 \int_1^{S_0} \left\{ \frac{(S-1)^{2p+1}}{S^3} - \frac{1}{(p+1)} \frac{(S-1)^{2p+2}}{S^4} \right\} dS \end{aligned} \quad (50)$$

where

$$\theta_0 = \frac{m \ell V^2}{12 M_0} \frac{(3+6K)^2}{(2+6K)}$$

is the damage angle which would be obtained if the beam were ideally plastic. Substitution of (49) into (50) gives

$$\frac{\theta_f}{\theta_o} = 2(p+1) \frac{s_o^2}{(s_o - 1)^{2p+2}} \int_1^{s_o} \left(\frac{(s-1)^{2p+1}}{s^3} - \frac{1}{(p+1)} \frac{(s-1)^{2p+2}}{s^4} \right) ds \quad (51)$$

By integrating the second term in the integral by parts we obtain

$$\frac{\theta_f}{\theta_o} = \frac{2}{3s_o} + \frac{2(p+1)s_o^2}{3(s_o - 1)^{2p+2}} \int_1^{s_o} \frac{(s-1)^{2p+1}}{s^3} ds \quad (52)$$

If $2p+1$ is integral, then the integration of (52) is elementary. However the results are not suitable for computation and a better procedure is the following. By introducing a new dummy variable

$$u = \frac{s_o - s}{s_o - 1}$$

(52) is reduced to

$$\frac{\theta_f}{\theta_o} = \frac{2}{3s_o} + \frac{2(p+1)}{3s_o} \int_0^1 (1-u)^{2p+1} \left[1 - u \left(\frac{s_o - 1}{s_o} \right) \right]^{-3} du$$

Expansion of $\left[1 - u \left(\frac{s_o - 1}{s_o} \right) \right]^{-3}$ by the binomial theorem then gives

$$\frac{\theta_f}{\theta_o} = \frac{2}{3s_o} + \frac{2(p+1)}{3s_o} \int_0^1 (1-u)^{2p+1} \sum_{n=0}^{\infty} \frac{(n+2)(n+1)}{2} \left(\frac{s_o - 1}{s_o} \right)^n u^n du \quad (53)$$

For $0 \leq u \leq 1$, the series above converges uniformly for $\frac{1}{2} < s_o < \infty$. This range includes all physically possible values of s_o . Interchange of the order of summation and integration in (53) yields

$$\frac{\theta_f}{\theta_0} = \frac{2}{3S_0} + \frac{2p+2}{3S_0} \sum_{n=0}^{\infty} \frac{(n+2)(n+1)}{2} \left(\frac{S_0-1}{S_0}\right)^n \int_0^1 (1-u)^{2p+1} u^n du$$

Using the known result

$$\int_0^1 u^{a-1} (1-u)^{b-1} du = \frac{\Gamma(a)\Gamma(b)}{\Gamma(a+b)}$$

we obtain

$$\begin{aligned} \frac{\theta_f}{\theta_0} &= \frac{2}{3S_0} + \frac{2p+2}{3S_0} \sum_{n=0}^{\infty} \frac{(n+2)(n+1)}{2} \left(\frac{S_0-1}{S_0}\right)^n \frac{\Gamma(n+1)\Gamma(2p+2)}{\Gamma(2p+n+3)} \\ &= \frac{1}{S_0} \left\{ 1 + \frac{1}{6} \sum_{n=1}^{\infty} \frac{\Gamma(n+3)\Gamma(2p+3)}{\Gamma(2p+n+3)} \left(\frac{S_0-1}{S_0}\right)^n \right\} \end{aligned} \quad (54)$$

The series in (54) converges rapidly and is suitable for numerical calculation. Note p need not be integral. Equations (49) and (54) are parametric equations relating the damage angle θ_f to the impact velocity V , through the parameter S_0 . This relationship is shown in figure 11. Experimental results from reference [3] are also shown for comparison. In plotting the experimental points the same value of β was used as was used in drawing figure 5.

We note that the theory predicts a sharp drop in the damage angle due to the strain-rate effect. Over most of the range of velocities the damage angle is about half that predicted by the rigid-ideally plastic theory, which is in rough agreement with experimental results. The experimental points all lie below the theoretical curves, and this might be attributed to the effect of strain-hardening which we have not

considered here.

Three parameters appear in the stress-strain relation, namely p , M_0 (or σ_0), and β . In the curve of damage angle vs. non-dimensional impact velocity the parameter M_0 enters only in the scale factor of the ordinate Θ_f/Θ_0 , while the parameter β enters only in the scale factor of the abscissa $\frac{Vc}{\beta l^2} \left(\frac{3+6\nu}{2+6\nu} \right)^2$. Only the exponent p affects the shape of the curve. Figure 11 indicates that the curve is rather insensitive to changes in the value of p .

Changes in the value of β would have the effect of shifting plotted experimental points to the right or left in figure 11. Since the curves are rather flat over most of the range, changes in the value of β would do little to move experimental points closer to or farther from the theoretical curves. Thus the agreement between theory and experiment would be influenced little by inaccuracies in the value of β . The ordinate Θ_0/Θ_f , however involves M_0 (or σ_0) directly. Changes in M_0 would have the effect of moving plotted experimental points upward or downward, and this would strongly affect any agreement or disagreement between theory and experiment.

Therefore, in the present theory, the most critical parameter is M_0 (or σ_0); the others seem to be rather unimportant.

4.2. Calculation of Maximum Plastic Strain

The strain is calculated from

$$\epsilon = \int_0^t \dot{\epsilon} dt \quad (55)$$

At the root of the beam

$$\dot{\epsilon}_m = \dot{\kappa}_m c = \beta \left(\frac{M_m}{M_0} - 1 \right)^p$$

from (42). This is the greatest strain-rate within the plastic region. Then we have

$$\begin{aligned} \epsilon_m &= \beta \int_0^t \left(\frac{M_m}{M_0} - 1 \right)^p dt \\ &= \beta \int_0^{\theta_f} (S - 1)^p \frac{d\epsilon}{\dot{\epsilon}} \end{aligned}$$

since $dt = d\theta/\dot{\epsilon}$. Hence, using (44) and (48),

$$\epsilon_m = \frac{\pi c V^2}{6 M_0^2} \frac{(2 + 6K)^2}{(3 + 6K)^2} \int_1^{S_0} \left\{ \frac{(S - 1)^{2p}}{S^2} - \frac{1}{(p + 1)} \frac{(S - 1)^{2p+1}}{S^3} \right\} dS \quad (56)$$

The procedure used to evaluate (56) is essentially the same as the procedure used to evaluate (51). Going directly to the final result,

$$\epsilon_m = \frac{\pi c V^2}{12 M_0^2} \frac{(3 + 6K)^3}{(2 + 6K)^2} \frac{(p + 1)}{(S_0 - 1)} \left\{ 1 + \sum_{n=0}^{\infty} \left(\frac{S_0 - 1}{S_0} \right)^n \frac{\Gamma(n+2)\Gamma(2p+1)}{\Gamma(2p + n + 2)} \right\} \quad (57)$$

(57) has been evaluated using values of the parameters appropriate to the mild-steel beams used in the experiments of Mentel,

Green, and Symonds [3], [4]. Also, the values of p and β used in plotting figure 5 were adopted. The results are shown in figure 12.

Note that the strain calculated here is the strain at the root of the beam, which is the maximum strain. The average strain in the plastically deformed section of the beam is, of course, less than this.

It is seen from figure 12 that the curves of ϵ_m vs. V are very closely straight lines on a logarithmic scale. This suggests that the $\epsilon_m - V$ relation can be approximated by a power law. Using only the first term of the series (57) we have

$$\epsilon_m \approx \frac{mcV^2}{24M_0} \frac{(3 + 6K)^3}{(2 + 6K)^2} \frac{(2p + 3)}{(S_0 - 1)} \quad (58)$$

From (49)

$$(S_0 - 1) = \left[\frac{(p + 1)Vc}{\beta l^2} \left(\frac{3 + 6K}{2 + 6K} \right)^2 \right]^{\frac{1}{p+1}} S_0^{\frac{1}{p+1}} \quad (59)$$

Use the value $p = 5$. Then substitution of (59) into (58) gives

$$\epsilon_m \approx \frac{mc^{5/6} \beta^{1/6} l^{1/3}}{2.49M_0} \cdot \frac{(3 + 6K)^{8/3}}{(2 + 6K)^{5/3}} \frac{V^{11/6}}{S_0^{1/6}} \quad (60)$$

The range of interest of S_0 is $1.6 \leq S_0 \leq 2.0$ roughly. In this range $S_0^{1/6}$ varies by only 4%. Hence, putting $S_0^{1/6} \approx 1.8^{1/6} = 1.103$ in (60) we obtain

$$\epsilon_m \approx \frac{mc^{.83} \beta^{.167} l^{.33} (3 + 6K)^{2.67}}{2.74M_0 (2 + 6K)^{1.67}} V^{1.83} \quad (61)$$

as an approximate formula for the maximum strain.

4.3. Calculation of Strain Rates

At the root of the beam

$$\dot{\epsilon}_m = \dot{\epsilon}_c = \beta \left(\frac{M_m}{M_0} - 1 \right)^p = \beta (S - 1)^p$$

from (42). The maximum strain-rate occurs at the beginning of the deformation (when S is largest) and hence is

$$\dot{\epsilon}_{MAX} = \beta (S_0 - 1)^p \quad (62)$$

Equations (49) and (62) give a parametric relation between maximum strain-rate and impact velocity.

Again an approximate formula can be developed. Substitution of (59) into (62) yields

$$\dot{\epsilon}_{MAX} = \beta^{\frac{1}{p+1}} \left[\frac{(p+1)VcS_0}{l^2} \left(\frac{3+6K}{2+6K} \right)^2 \right]^{\frac{p}{p+1}}$$

Taking $p = 5$, and using for S_0 its mean value 1.8, we obtain

$$\dot{\epsilon}_{MAX} \approx \frac{7.5\beta \cdot 167 \cdot c^{.83}}{1.67} \left(\frac{3+6K}{2+6K} \right)^{1.67} V^{.53} \quad (63)$$

The mean strain rate, i.e. the time average strain rate, at the root of the beam is

$$\dot{\epsilon}_{MLN} = \frac{\int \dot{\epsilon}_m dt}{\int dt} = \frac{\epsilon_m}{\int dt} \quad (64)$$

where the integration is taken over the interval during which plastic deformation occurs. ϵ_m has already been evaluated. Now

$$\begin{aligned} \int dt &= \int \frac{dS}{\dot{S}} \\ &= \frac{m^4 \beta}{6M_0 c} \frac{(2+6K)^2}{(3+6K)} \int_1^{S_0} \left\{ \frac{(S-1)^p}{S^2} - \frac{1}{(p+1)} \frac{(S-1)^{p+1}}{S^3} \right\} dS \quad (65) \end{aligned}$$

by using (44) and (48). The integral (65) can be evaluated by the same procedure used in evaluating (51). The result is

$$\int dt = \frac{m \ell^2 v (3+6K)}{12M_0} \cdot \frac{1}{S_0} \left\{ 1 + \sum_{n=0}^{\infty} \frac{\Gamma(n+2)\Gamma(p+2)}{\Gamma(n+p+2)} \left(\frac{S_0-1}{S_0}\right)^n \right\} \quad (66)$$

Substitution of (66) and (57) into (64) yields

$$\begin{aligned} \dot{\epsilon}_{\text{MEAN}} &= \frac{V_0}{\ell^2} \left(\frac{3+6K}{2+6K}\right)^2 \frac{(p+1)S_0}{(S_0-1)} \frac{\left\{ 1 + \sum_{n=0}^{\infty} \frac{\Gamma(n+2)\Gamma(2p+1)}{\Gamma(2p+n+2)} \left(\frac{S_0-1}{S_0}\right)^n \right\}}{\left\{ 1 + \sum_{n=0}^{\infty} \frac{\Gamma(n+2)\Gamma(p+2)}{\Gamma(n+p+2)} \left(\frac{S_0-1}{S_0}\right)^n \right\}} \\ &= \dot{\epsilon}_{\text{MAX}} \frac{\left\{ 1 + \sum_{n=0}^{\infty} \frac{\Gamma(n+2)\Gamma(2p+1)}{\Gamma(2p+n+2)} \left(\frac{S_0-1}{S_0}\right)^n \right\}}{\left\{ 1 + \sum_{n=0}^{\infty} \frac{\Gamma(n+2)\Gamma(p+2)}{\Gamma(n+p+2)} \left(\frac{S_0-1}{S_0}\right)^n \right\}} \quad (67) \end{aligned}$$

in view of (62) and (49).

In figure 13, numerical results for $\dot{\epsilon}_{\text{MAX}}$ and $\dot{\epsilon}_{\text{MEAN}}$ are shown. We note that, within the range of velocities considered, $\dot{\epsilon}_{\text{MEAN}}$ is very nearly one-half of $\dot{\epsilon}_{\text{MAX}}$.

4.4. Length of Plastic Zone

From (40),

$$\frac{x_n}{\ell} = \left(\frac{2+6K}{3+6K}\right) \frac{S_0-1}{S_0}$$

The maximum value of x_n/ℓ occurs at the beginning of the motion, and is

$$\max\left(\frac{x_n}{\ell}\right) = \left(\frac{2+6K}{3+6K}\right) \frac{S_0-1}{S_0} \quad (68)$$

The mean value of x_n/ℓ , i.e. the time average of x_n/ℓ is given by

$$\text{mean}\left(\frac{x_n}{\ell}\right) = \frac{\int \frac{x_n}{\ell} dt}{\int dt} \quad (69)$$

The expression (69) can be evaluated in the same way as the expression (64) for the mean strain-rate was evaluated. Going directly to the final result,

$$\begin{aligned} \text{mean}\left(\frac{x_n}{\ell}\right) &= \frac{(2+6K)}{3+6K} \frac{2(S_0-1)}{S_0} \cdot \frac{\left\{ 1 + \frac{(2p+1)}{5} \sum_{n=0}^{\infty} \frac{\Gamma(n+3)\Gamma(p+2)}{\Gamma(n+p+3)} \left(\frac{S_0-1}{S_0}\right)^n \right\}}{\left\{ 1 + \sum_{n=0}^{\infty} \frac{\Gamma(n+2)\Gamma(p+2)}{\Gamma(n+p+2)} \left(\frac{S_0-1}{S_0}\right)^n \right\}} \\ &= \text{max}\left(\frac{x_n}{\ell}\right) \cdot \frac{2}{3} \cdot \frac{\left\{ 1 + \frac{(2p+1)}{5} \sum_{n=0}^{\infty} \frac{\Gamma(n+3)\Gamma(p+2)}{\Gamma(n+p+3)} \left(\frac{S_0-1}{S_0}\right)^n \right\}}{\left\{ 1 + \sum_{n=0}^{\infty} \frac{\Gamma(n+2)\Gamma(p+2)}{\Gamma(n+p+2)} \left(\frac{S_0-1}{S_0}\right)^n \right\}} \end{aligned} \quad (70)$$

In figure 14, $\text{max}(\frac{x_n}{\ell})$ and $\text{mean}(\frac{x_n}{\ell})$ are plotted against the non-dimensional impact velocity. It is seen that, according to the present theory, the mean value of x_n/ℓ is about 1/4 over most of the range of velocities, and that the peak value of x_n/ℓ can be as high as 1/2. Therefore it appears that the basic assumption $x_n/\ell \ll 1$ is satisfied only in a very crude manner, and consequently the accuracy of the present theory is questionable.

5. Discussion of results

The foregoing analyses were based on the assumption, among others, that the length of the plastic zone is short compared with the length of the beam. All test results with both mild steel and aluminum alloy specimens, described in references [3] and [4], indicate this assumption to be correct. The region of large plastic deformation occurs in a length approximately 0.5 in. or less, so that experimentally $x_n/\ell \leq 0.1$. However the analysis developed in this report, which is based on this assumption, predicts that under the conditions realized in many of the tests the value of x_n/ℓ is actually so large as to invalidate the theory. The reasons for this are not yet understood, and the analysis is unsatisfactory to this extent. The discrepancy may perhaps be due to the use of stress-strain or stress-strain rate relations which are unsatisfactory, since it is by no means certain that stress-strain data obtained by Manjoine [6] for high strain rates can be applied to problems of bending in the manner done here. Further development of the theory with a view to removing the assumption $x_n \ll \ell$ is desirable.

Both the analyses accounting for strain-hardening and strain-rate sensitivity separately, predict that the damage angle is considerably less than the angle calculated on the basis of a rigid-ideally plastic material. Of the two effects, strain-rate sensitivity appears to be the more important, and this conclusion is strengthened by the findings of Manjoine [6] that the stress-strain curve becomes flatter at higher strain-

rates. The reduction in damage angle due to either strain-hardening or strain-rate sensitivity, by itself, is not sufficient to bring the theoretical analysis into agreement with experimental results. From the magnitudes of the reductions due to the two separate effects, however, it seems likely that agreement could be obtained by considering the combination of the two effects. This has previously been stated by Mentel [3]. Thus it would be desirable to extend the present analysis so that strain-hardening and strain-rate sensitivity are accounted for simultaneously.

That an extension of the analysis in this direction is desirable is evident also from the curves of strain and strain-rate vs. impact velocity. Thus, the predicted mean strain-rates in a strain-hardening beam are so large that the neglect of strain rate effects is not justified. On the other hand, predicted strains in rate-sensitive beams are so large that some account should be taken of strain-hardening, even though its importance diminishes at high rates of strain.

References

1. E. H. Lee and P. S. Symonds, "Large Plastic Deformations of Beams under Transverse Impact". Trans. ASME, Vol. 19, pp. 308-314, 1952.
2. P. S. Symonds and C. F. A. Leth, "Impact of Finite Beams of Ductile Metal". Jour. of Mech. and Phys. of Solids, Vol. 2, pp. 92-102, 1954.
3. T. J. Mentel, "The Plastic Deformation due to Impact of a Cantilever Beam with an Attached Tip Mass". Tech. Report No. 8 from Brown University to Office of Ordnance Research under contract DA-19-020-ORD-3172, March, 1956.
4. P. S. Symonds, D. S. Green, and T. J. Mentel, "Plastic Deformation of Beams in Impact - Theory and Preliminary Tests". Report of Brown University to Office of Naval Research under contract N7onr-35801, in preparation.
5. E. W. Parkes, "The Permanent Deformation of a Cantiliver Struck Transversely at its Tip". Proc. Royal Society Series A, Vol. 228, pp. 462-476, 1955.
6. M. J. Manjoine, "Influence of Rate of Strain and Temperature on Yield Stresses of Mild Steel". Jour. Appl. Mech. Vol. 11, p. 211, 1944.
7. L. E. Malvern, "Plastic Wave Propagation in a Bar of Material Exhibiting a Strain Rate Effect". Quart. Appl. Math. Vol. VIII, No. 4, p. 405, 1951.

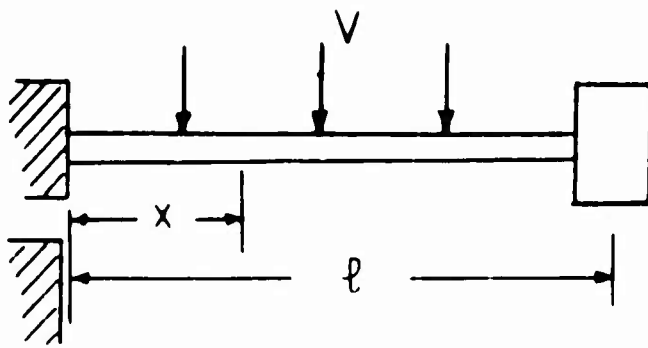


FIG. 1

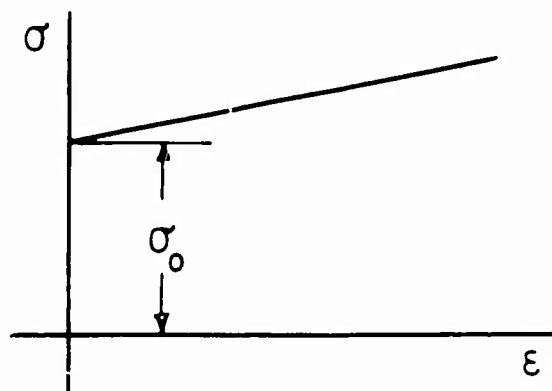


FIG. 2

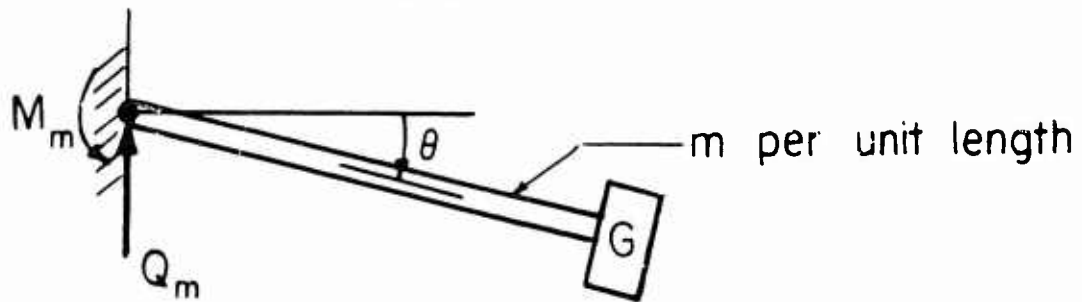


FIG. 3

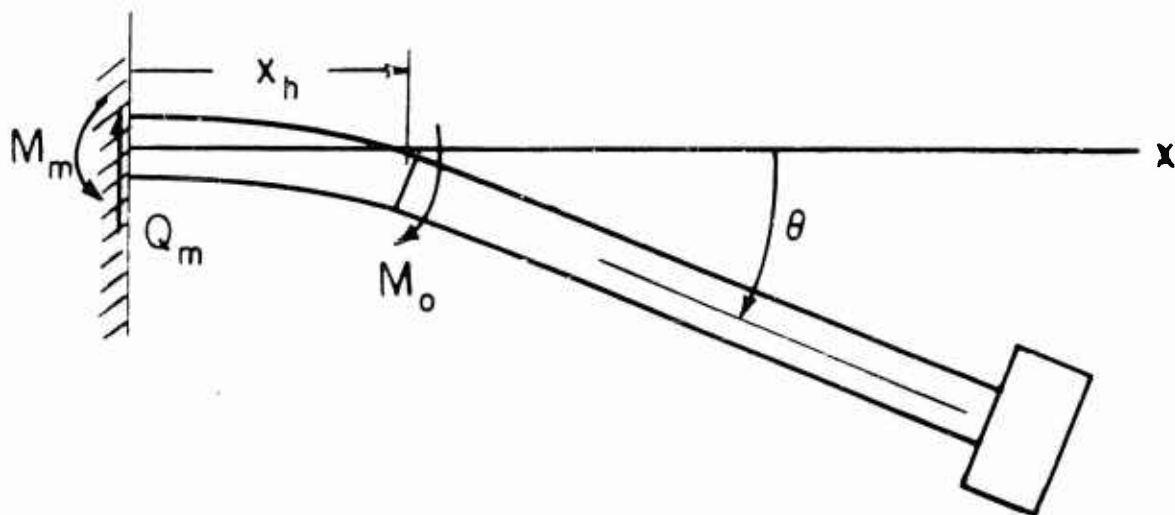


FIG. 4

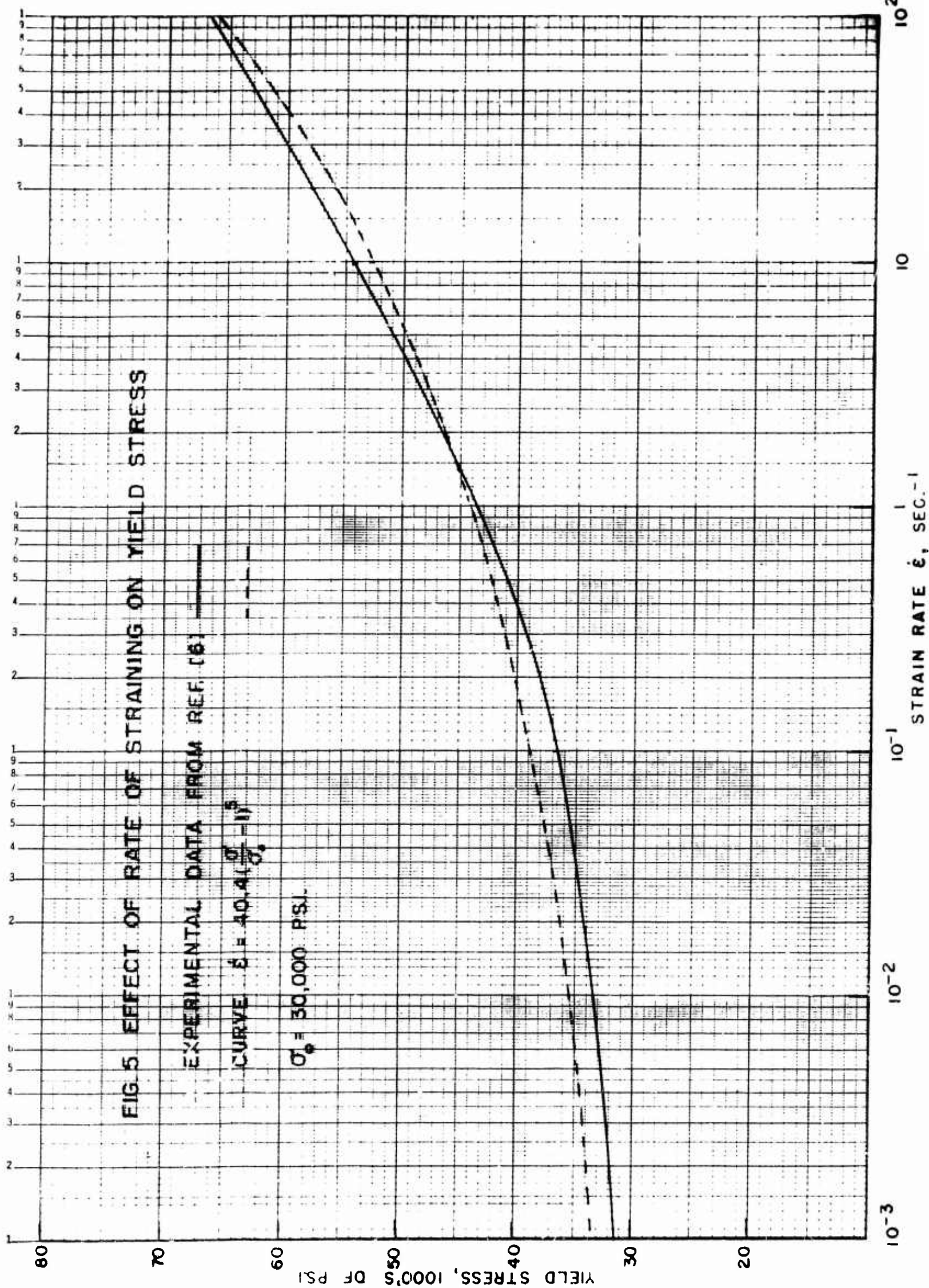
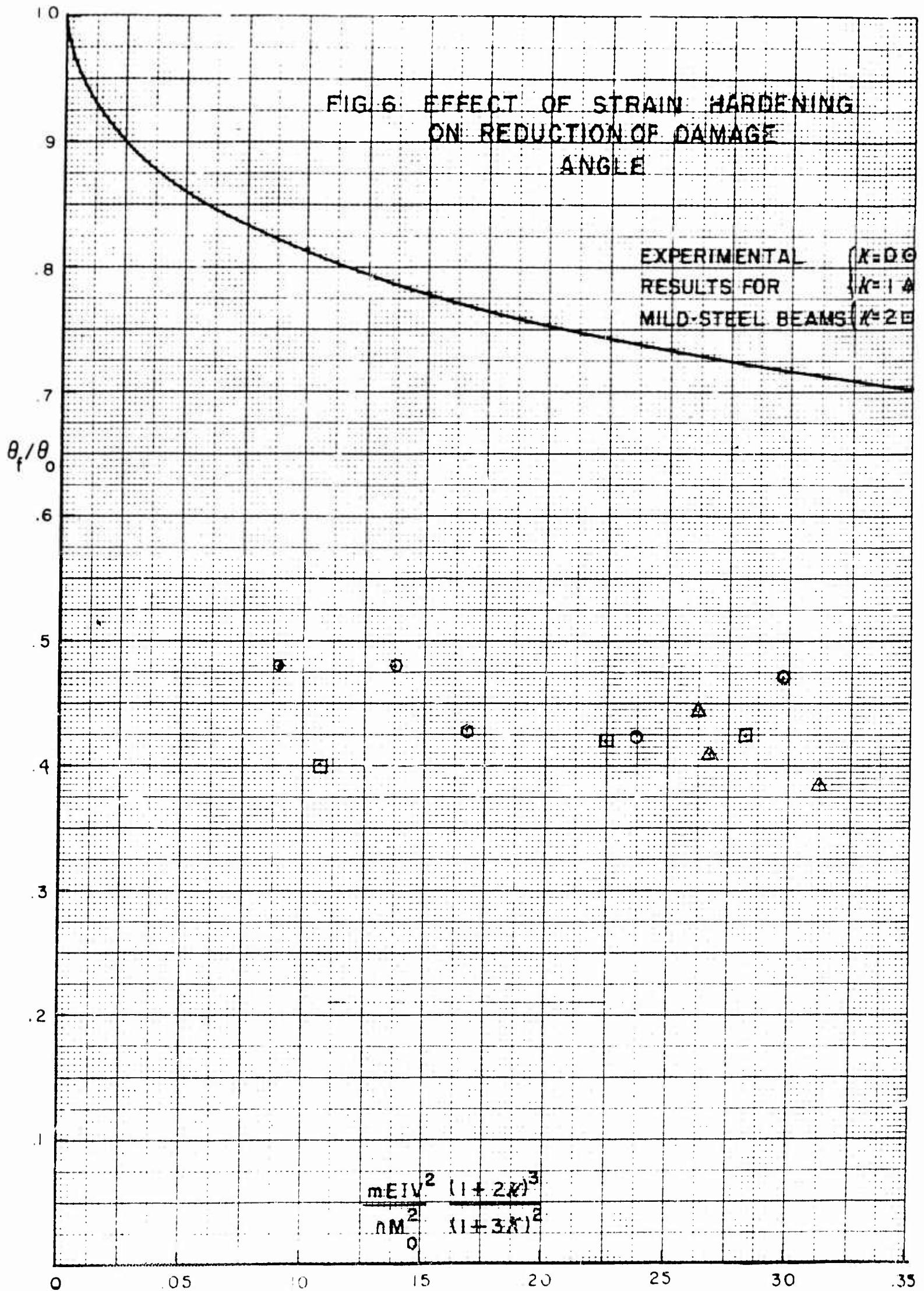


FIG. 6 EFFECT OF STRAIN HARDENING
ON REDUCTION OF DAMAGE
ANGLE



$$\frac{(1+2K)^3}{(1+3K^2)(1+K)}$$

K·E 10 X 10 TO THE 1/2 INCH 359-11K
KEUFFEL & ESSER CO. MADE IN U.S.A.

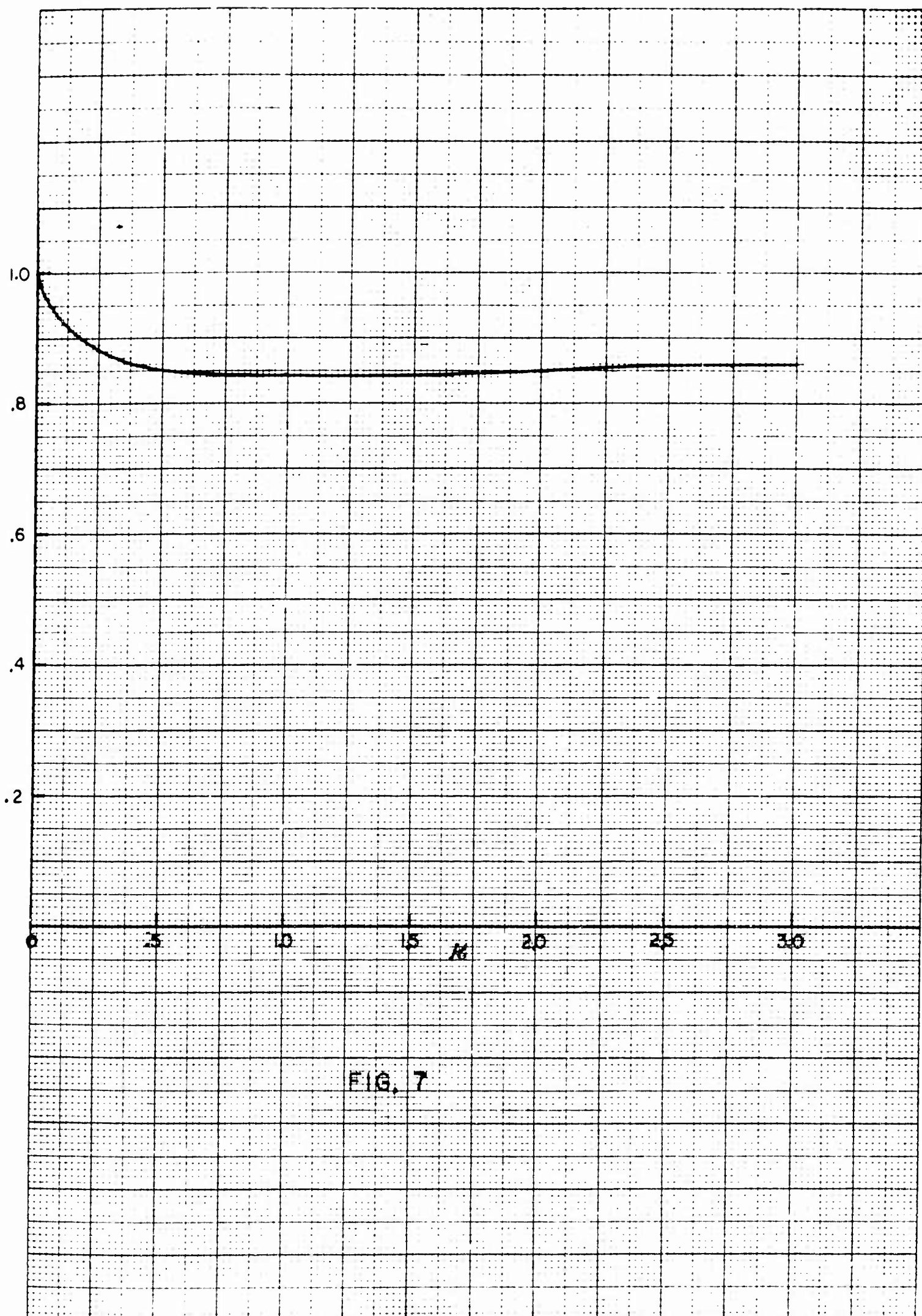


FIG. 7

FIG 8 PREDICTED STRAINS IN STRAIN-HARDENING MILD STEEL BEAMS

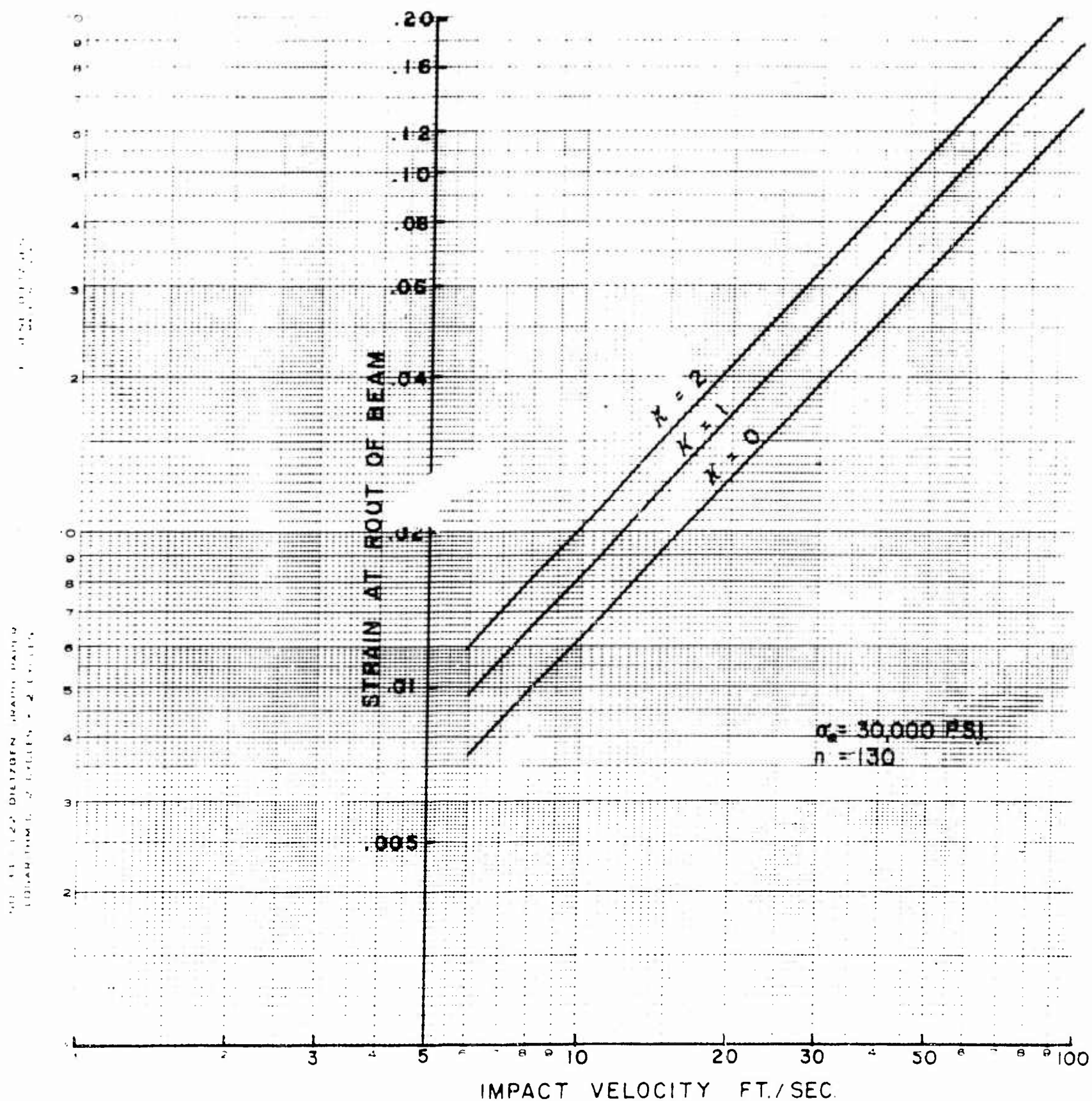


FIG. 9 PREDICTED MEAN STRAIN-RATES IN STRAIN-HARDENING MILD-STEEL BEAMS

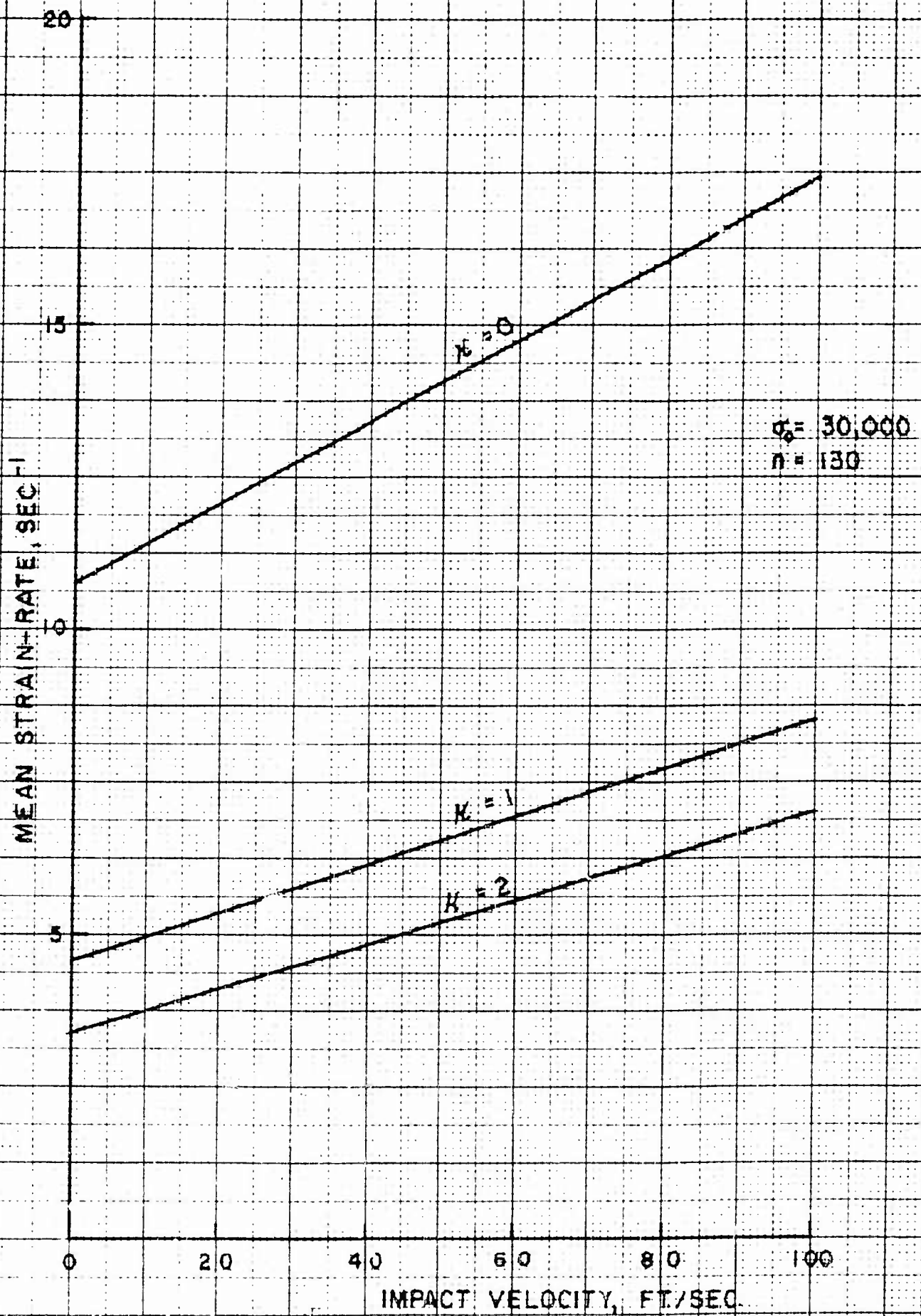


FIG. 10 LENGTH OF PLASTIC REGION — WORK-HARDENING BEAM

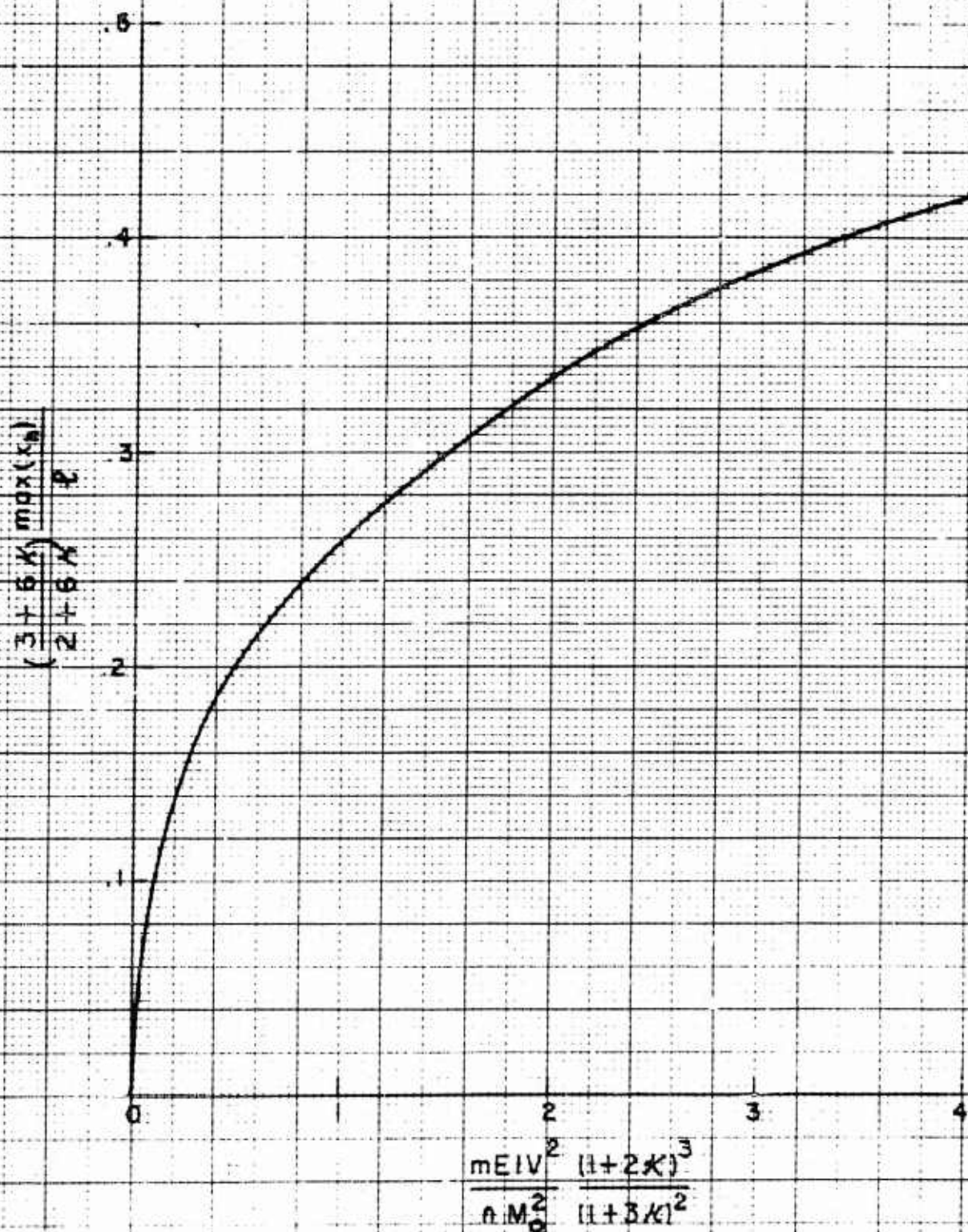


FIG. II DAMAGE CURVES FOR
RATE SENSITIVE BEAMS

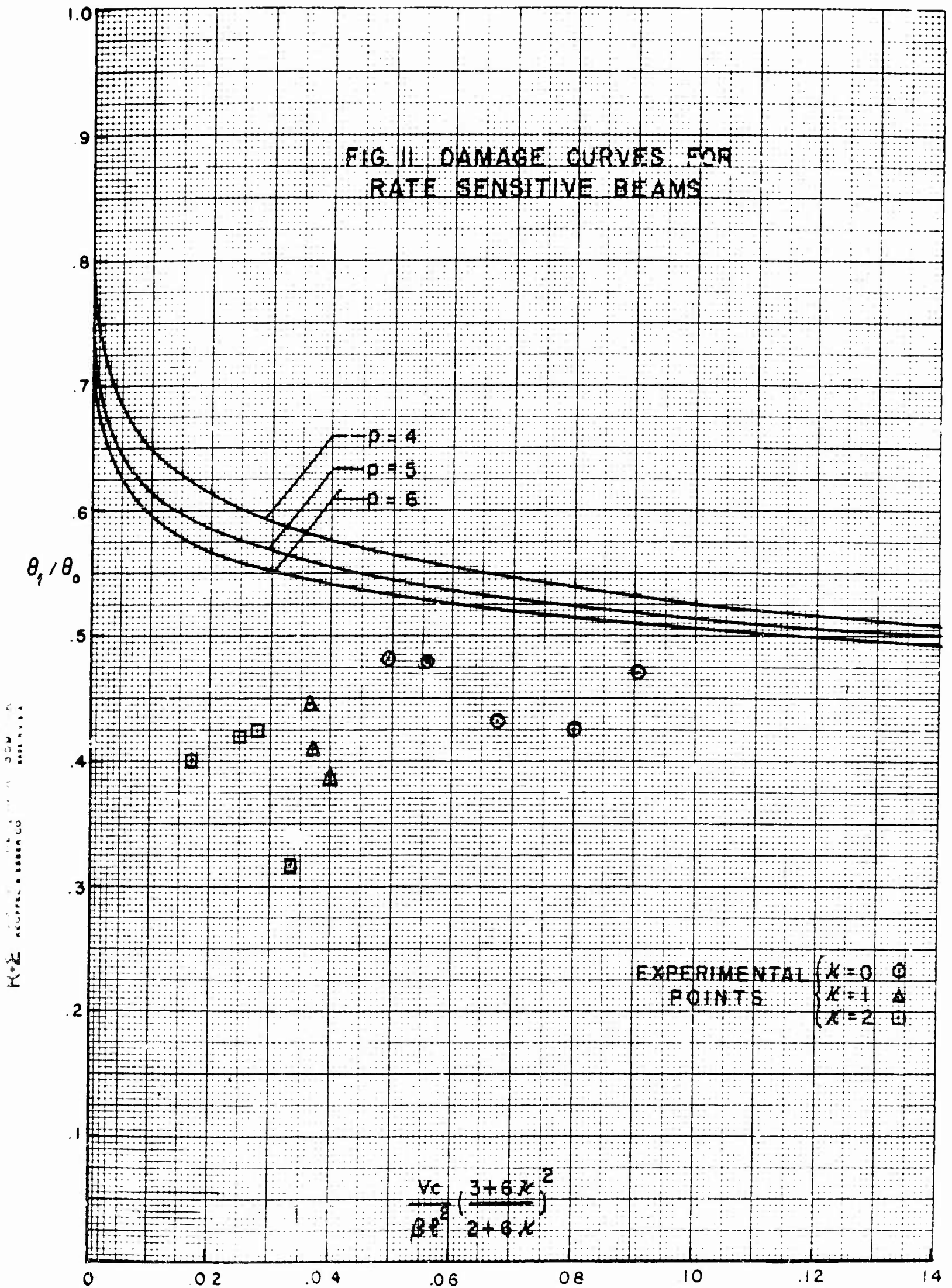


FIG 12 PREDICTED STRAINS IN EXPERIMENTAL MILD
STEEL BEAMS, ACCOUNTING FOR
STRAIN-RATE SENSITIVITY

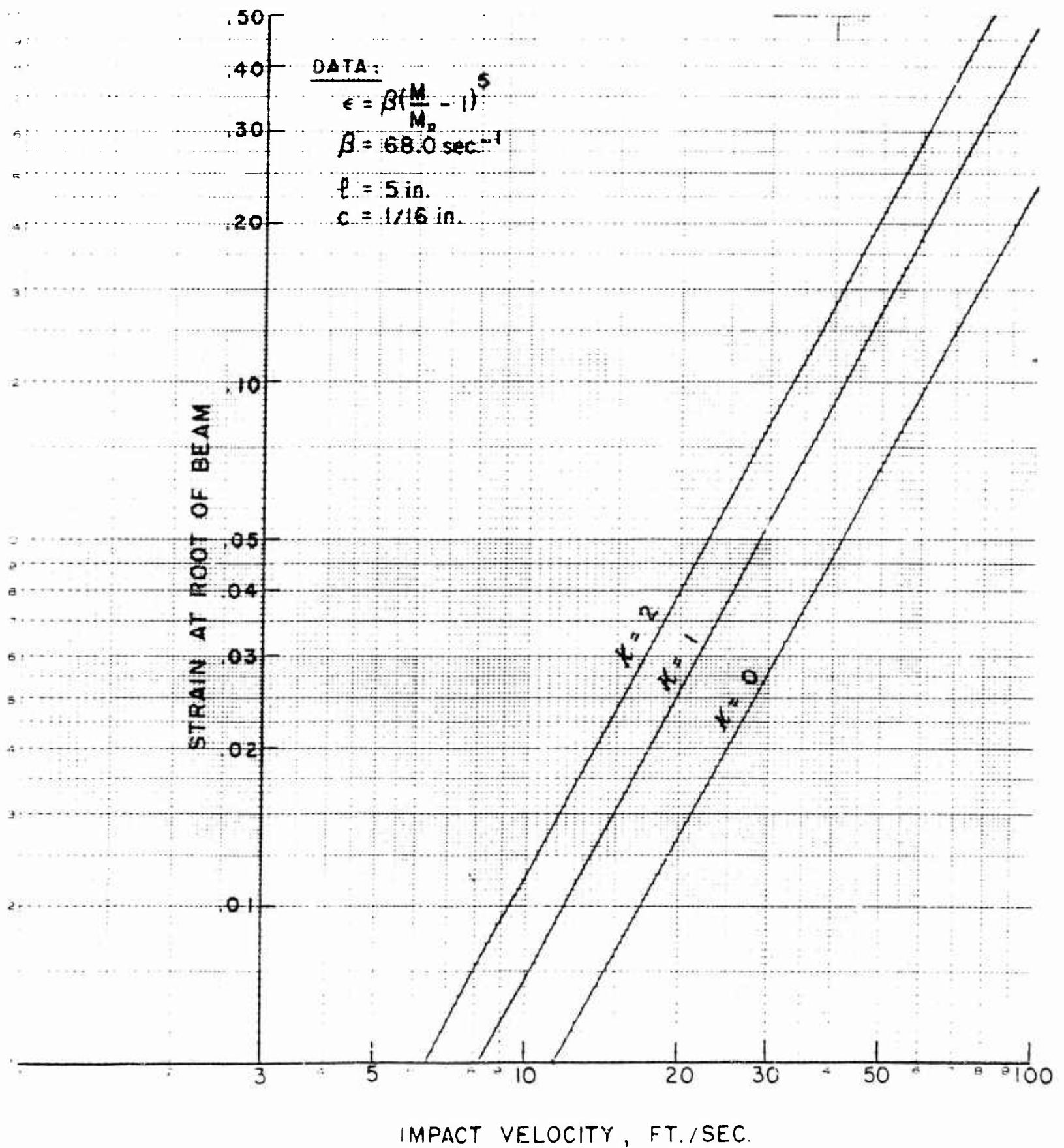


FIG 13 PREDICTED STRAIN-RATES IN EXPERIMENTAL
MILD STEEL BEAMS, ACCOUNTING FOR
STRAIN-RATE SENSITIVITY

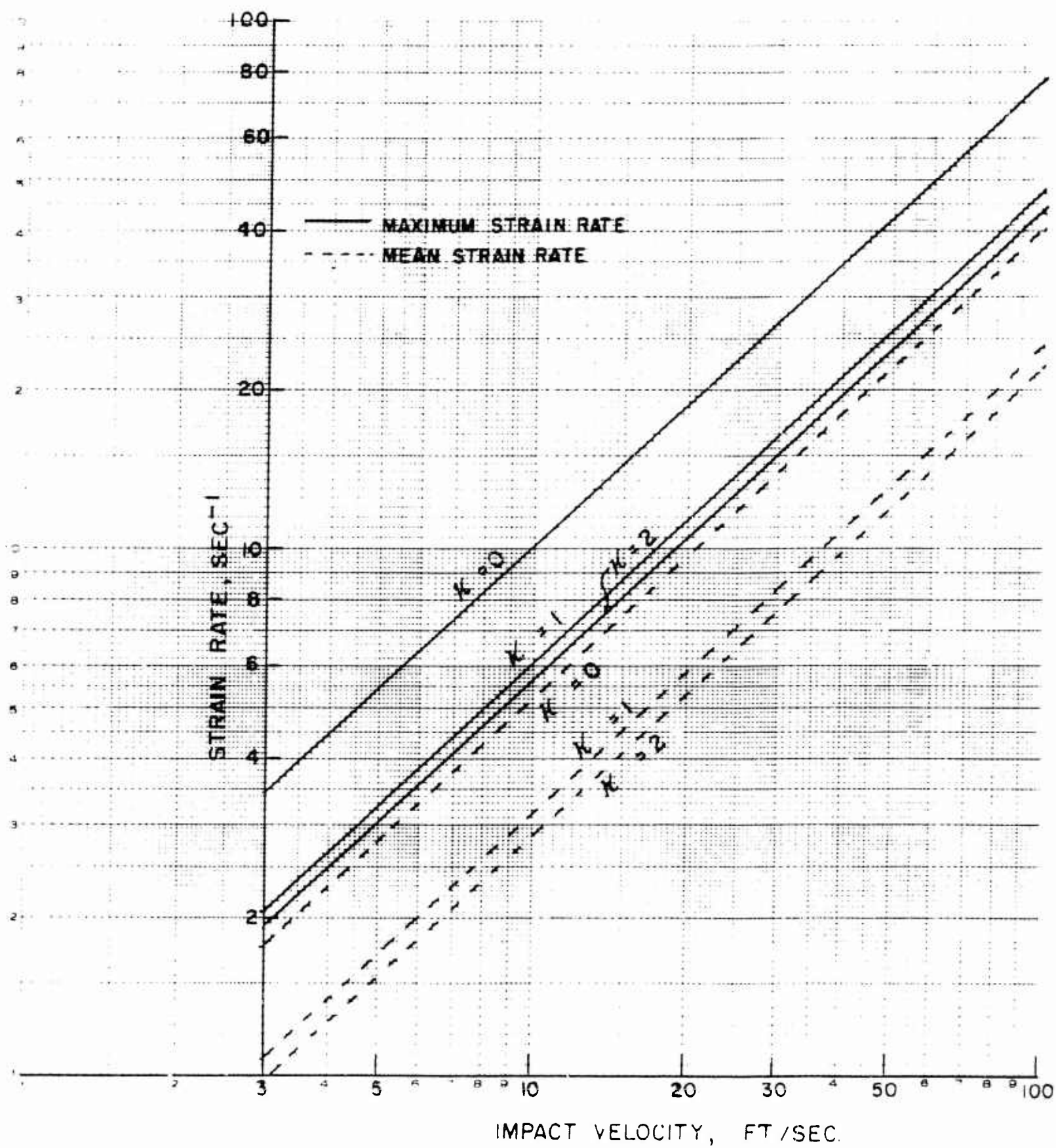


FIG. 14 LENGTH OF PLASTIC REGION

